Heterogeneous Catalysis

International Edition: DOI: 10.1002/anie.201900013
German Edition: DOI: 10.1002/ange.201900013

Confinement Effects in Zeolite-Confined Noble Metals

Si-Ming Wu, Xiao-Yu Yang, and Christoph Janiak*

Keywords:
cascade reactions · confined catalysis · confined synthesis · noble metal · zeolite

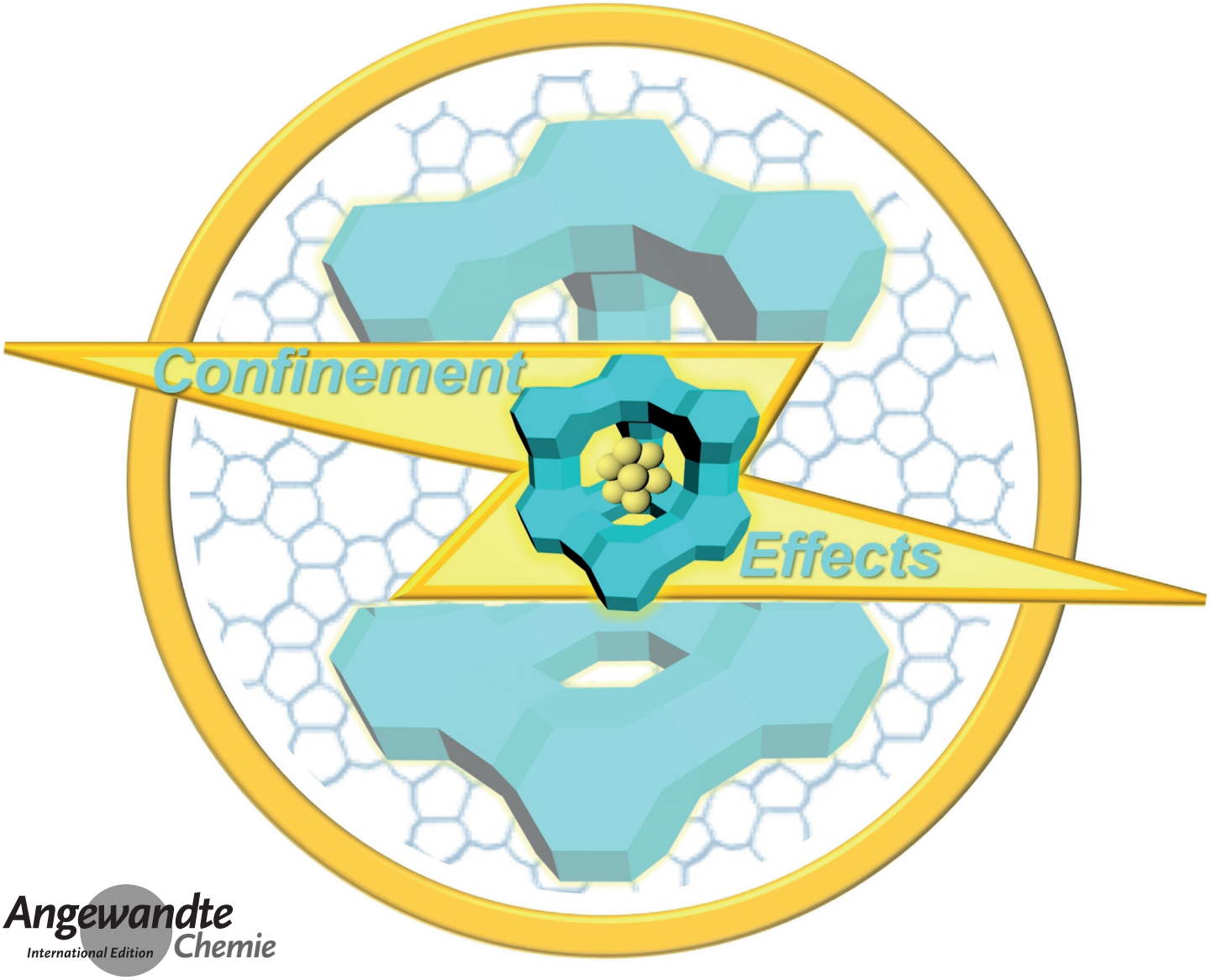

Confinement of noble nanometals in a zeolite matrix is a promising way to special types of catalysts that show significant advantages in size control, site adjustment, and nano-architecture design. The beauty of zeolite-confined noble metals lies in their unique confinement effects on a molecular scale, and thus enables spatially confined catalysis akin to enzyme catalysis. In this Minireview, the confined synthesis strategies of zeolite-confined noble metals will be briefly discussed, showing the processes, advantages, features, and mechanisms. The confined catalysis carried on zeolite-confined noble metals will be summarized, and great emphasis will be paid to the confinement effects involving size, encapsulation, recognition, and synergy. Great progress of atomic sites in the size effect, supercage stabilization in the encapsulation effect, site adsorption in the recognition effect, and cascade reaction in the synergy effect are highlighted. This Minireview is concluded with challenges and opportunities in terms of the synthesis of zeolite-confined noble metals and their applications to design multifunctional catalysts with high catalytic activity, selectivity, and stability.

1. Introduction

The noble metals ruthenium, rhodium, palladium, iridium, platinum, gold, and silver have been considered as most efficient catalysts for industrial catalysis, energy conversion, and environmental treatment.[1–5] Nano- and atomic size effects have attracted great interest for the design of high-performance nanometal catalysts, owing to the high surface-to-volume atom ratio, the high exposure of active facets, and large number of low coordination or unsaturated sites.[6–8] However, the nanometals at the nano-/atomic scale are not in a thermodynamically but only in a more or less kinetically stable state, although many successful approaches have been attempted towards increased kinetic stabilization such as organic/inorganic capping,[9–11] long-range organizing,[12,13] and hetero compositing.[14,15] For practical application and structural stability, porous materials are most widely used as supports to nanometal dispersions, for interaction enhancement and cost decrease.[16,17] Many porous supports, such as carbons,[18–20] polymers,[21,22] oxides,[8,23] and zeolites, have been used for the confined synthesis for size control, facet adjustment and morphology fabrication of noble metals. The beauty of such confined synthesis lies in the fact that strong interactions of the nanometals with the porous support can prevent nano-aggregation.[24,25] Advantageous features of nano-architectures allow for high accessibility and corresponding confined catalysis, by creating stable, finely dispersed metal clusters with a high catalytic activity, as well as a low consumption of the noble metal.

It is therefore highly attractive to develop a powerful tool for controllable synthesis of uniform nanometals in porous systems. The varieties of supports often result in different synthesis strategies for confining nanometals and specific application, such as high-temperature treatment to carbon-supported electrocatalysts,[19,20] defect engineering to oxide-supported photocatalysts,[26–28] and ligand coordination to polymer-supported biocatalysts.[21,22] Zeolites, as promising porous supports, share core features as follows: 1) high surface area and strong interaction for stable dispersion of nanometals; 2) high physicochemical host stability for the structural integrity of the catalysts; 3) highly ordered structure for high catalytic selectivity; and 4) high feasibility to various metals for practical applications.[29–31]

Note that the specific adsorption sites in zeolites allow for the generation of nanoclusters of noble metals, creating a partition between the exterior surface and the interior pores.[7] Furthermore, the supercages in zeolites allow for the stabilization of unstable metal clusters, and offer an adjusting structure and volume to change the electronic configuration of nanometals,[32] whereby noble metals show very high catalytic activity and turnover frequency (TOF).[33–36] The so-called "noble" metals are usually very expensive metals and may constitute only about 1 wt% of the catalyst system, in which the noble metal is applied in a finely dispersed form as nanoparticles on a support (carrier).[2,37] Zeolite-confined nanometal clusters have now been prepared that are highly uniform and even down to the atomic scale, although work is needed to determine structures and properties with greater precision. These samples offer a long-awaited opportunity to enhance the catalytic gram-based activities of noble nanometals as less material is part of the inactive bulk phase. A vast array of synthesis methods, and corresponding structures have been

[*] S. M. Wu, Prof. X. Y. Yang
State Key Laboratory of Advanced Technology for Materials Synthesis and Processing, Wuhan University of Technology (WHUT)
Wuhan, 430070 (China)
E-mail: xyyang@whut.edu.cn
Prof. X. Y. Yang
Southern Marine Science and Engineering Guangdong Laboratory (Zhuhai) (SMSEGL) & School of Chemical Engineering and Technology
Sun Yat-sen University (SYSU)
Zhuhai, 519082 (China)
and
School of Engineering and Applied Sciences
Harvard University (HU)
Cambridge, MA 02138 (USA)
E-mail: xyyang@seas.harvard.edu.cn
Prof. C. Janiak
Institut für Anorganische Chemie und Strukturchemie
Heinrich-Heine-Universität Düsseldorf
40204 Düsseldorf (Germany)
The ORCID identification number(s) for the author(s) of this article can be found under:
https://doi.org/10.1002/anie.201900013.

developed in this area, mainly involving host–guest assembling of metal precursors into the preformed zeolites, re-transformation processing by recrystallization of low-crystalline, semi-crystalline, and amorphous nanostructured aluminosilicates and/or silica with dispersed metals nanoparticles/precursors, and direct synthesis by self-assembly of zeolite structural units and ligands of metal precursors during formation of zeolites nanocrystals.

The nature of aluminosilicates (zeolites) as a solid Lewis and Brønsted acid catalyst provides an opportunity to multiple-functional catalysts for applicability extension.[38] Some fascinating confinement effects and corresponding applications in catalysis due to the unique zeolite structures and supported noble metal nanocrystals were demonstrated, indicating that the design of both structures of zeolites and nanometals is of great importance in both academia and industry. Zeolite-confined nanosized noble metals have therefore been important nanocatalysts, being used on a large scale for the refining of petroleum, conversion of automobile exhaust, hydrogenation of carbon monoxide, hydrogenation of unsaturated fats, and many other processes.[39,40]

Owing to the strong scientific interest and practical importance of this field, a series of recent reviews on zeolite-supported metals have been published.[32,41,42] Each of these reviews addresses mainly structural aspects and their corresponding properties and applications. Thus, we felt that a mechanistic review on confinement effects from confined synthesis to confined catalysis would be informative. The analyses presented here have become feasible only relatively recently as advances in confined catalysis have started to provide access to the basis and core of zeolite-confined noble metals underpinning them. This Minireview will start from the confinement synthesis of zeolite-confined noble metals (Figure 1), showing the development, features, and mechanisms of different advanced synthesis strategies. First (Section 2), the approaches of host–guest assembly, re-transformation, and direct synthesis will be demonstrated, which succeed in confining metal cluster/nanoparticles within nanoarchitectures, and ultra-small atomic sites in the framework of zeolites. Next (Section 3), we will summarize the catalytic applications of zeolite-confined noble metals, and great emphasis will be paid to the confinement effects in catalysis (Figure 1), including size, encapsulation, recognition and synergy effects. The relationships between activity, stability, selectivity, and multi-functionality are illustrated in detail. Finally (Section 4), the important opportunities and challenges of zeolites-confined noble metals, including practical demand of the noble metals, hierarchical control of the zeolite structures, emerging need of catalysis applications, future requirement of mechanism extension, will be addressed to push forward the confined-catalysis applications. We hope that such a critical review can be helpful in achieving a better understanding of confined catalysis of noble metal nanoparticles in zeolites and show a promising way to the design of multifunctional catalysts with high catalytic activity, selectivity, and stability.

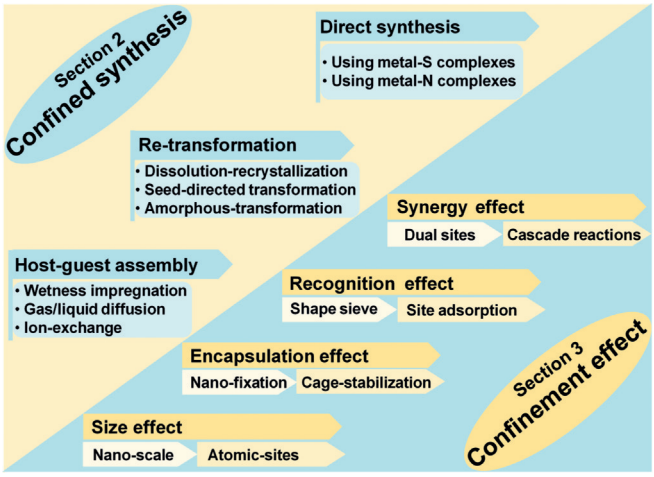

Figure 1. Brief summary of zeolite-confined noble metals from confined synthesis to confinement effects in confined catalysis.

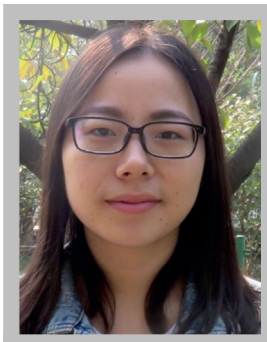

Si-Ming Wu received her BS (2013) and her Ph.D (2019) from Wuhan University of Technology (Co-education at University of Düsseldorf), under the supervision of Prof. Xiao-Yu Yang and Prof. Christoph Janiak. Her research mainly focuses on the design, synthesis, and applications of hierarchically porous materials.

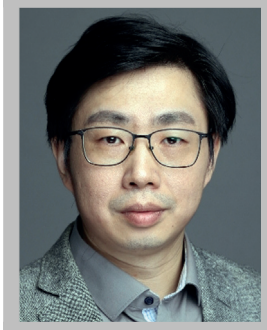

Xiao-Yu Yang received his Ph.D. from Jilin University (co-educated at FUNDP of Belgium). After a postdoctoral fellowship at the FUNDP, he worked as a "Chargé de Recherches" at the FNRS in Belgium. He is currently working as full professor at WHUT, co-professor at SMSEGL and SYSU, and visiting professor at HU. His research is aimed at hierarchical assembly techniques and hierarchical structured materials for the applications in energy, environment, catalysis, bioengineering, and ocean-engineering.

Christoph Janiak is full professor for Bioinorganic Chemistry and catalysis at the University of Düsseldorf, with research interests in the synthesis and properties of metal and porous organic frameworks (MOFs, COFs), metal nanoparticles, ionic liquids, and catalysis. Until 2018 he was a visiting professor at Wuhan University of Technology in China.

2. Confined Synthesis Strategies

Zeolite-supported noble metals were first reported in the 1970s as part of a protocol for limiting particle growth to a particular size regime as well as reducing particle aggregation.[43] Furthermore, by selecting and manipulating the

textural properties of zeolites, it should be possible to control the size and shape of the resulting nanoparticles in the pores/caves/channels of zeolites, as a so-called ship-in-bottle synthesis.[44–46] In 1995, Gates et al. thoroughly explained the spatial confinement of Y zeolite supported Ir and Pt nanoclusters.[32] Subsequently, a number of zeolites have been particularly interesting as the host network, such as FAU-type zeolites X and Y (12-membered-ring (MR) channel),[47] MFI-type zeolites (two 10-MR channels), and topologically related BEA (two 12-MR channels), SOD (6-MR channel), and LTA (8-MR channel) zeolite types.[48,49] At the beginning of the 21st century, with developments in nanoscale techniques and sol–gel chemistry, the nanometal units could be synthesized in nanostructured materials with a remarkable degree of control, which broke the limitation of pore size and provides instructions for confining larger-sized nanometal particles into nanostructures, such as core–shell structures.[50,51] Over the last decade, a great number of researchers have focused their attention on the development of strategies to prepare zeolite-confined noble metals.[41,42] Especially in the last five years, breakthroughs were made to confine nanometals into the zeolitic framework and ultra-small clusters into the wall of zeolites for the high-performance design of multifunctional catalysts.[33,52]

All synthesis strategies of zeolite-confined noble metals can be classified into the following three main approaches: 1) host–guest assembly of the preformed zeolites and metal precursors; 2) re-transformation of low/semi-crystalline and amorphous nanostructured supports with dispersed metal nanoparticles/precursors inside; and 3) direct synthesis using metal ligand precursors during the formation of zeolite nanocrystals. Herein, we identify the processes, advantages, features, and mechanisms of these confined synthesis strategies, as well as the detailed structures and descriptions of corresponding examples.

2.1. Host–Guest Assembly

The metal ions/complexes, as most used metal precursors, are generally introduced in zeolites by host–guest (preformed zeolites-metal precursors) assembling methods. Typical metal precursors are metal salts such as $PdCl_2$ for Pd, $RhCl_3$ for Rh, and metal complexes such as H_2PtCl_6, $Pt(acac)_2$ for Pt, $HAuCl_4$ for Au, $Pd(acac)_2$ for Pd, $Ir(CO)_2(acac)$ for Ir. These methods generally include wetness impregnation, gas/liquid diffusion, and ion-exchange (Figure 2a, left).

Wetness impregnation is often used to introduce the metal ions into almost all types of zeolites. A mixture of dehydrated support with a certain amount of solution containing metal precursors are prepared and dried, and then calcined and reduced under hydrogen flow to obtain the nanometals. Under such conditions, the amount of metal is not limited by the composition of the framework but by the pore volume and it is theoretically possible to completely fill the zeolite pores with metal precursors.[53] A typical preparation is that the introduction of metal salts or metal complexes into zeolites takes place in solution. This is followed by reduction with hydrogen to form metal clusters or nanoparticles, as well as sometimes oxidation for formation of fragmented species (so called mononuclear species).[29] This oxidation way has been successfully used to obtain site-isolated mononuclear noble metal catalysts.[54,55] Note that the exact nature of the formed species is often difficult to define. For example, extended X-ray absorption fine structure (EXAFS) results indicate the existence of a Pt-N, Pt-O, and Pt-Al coordination shell, which

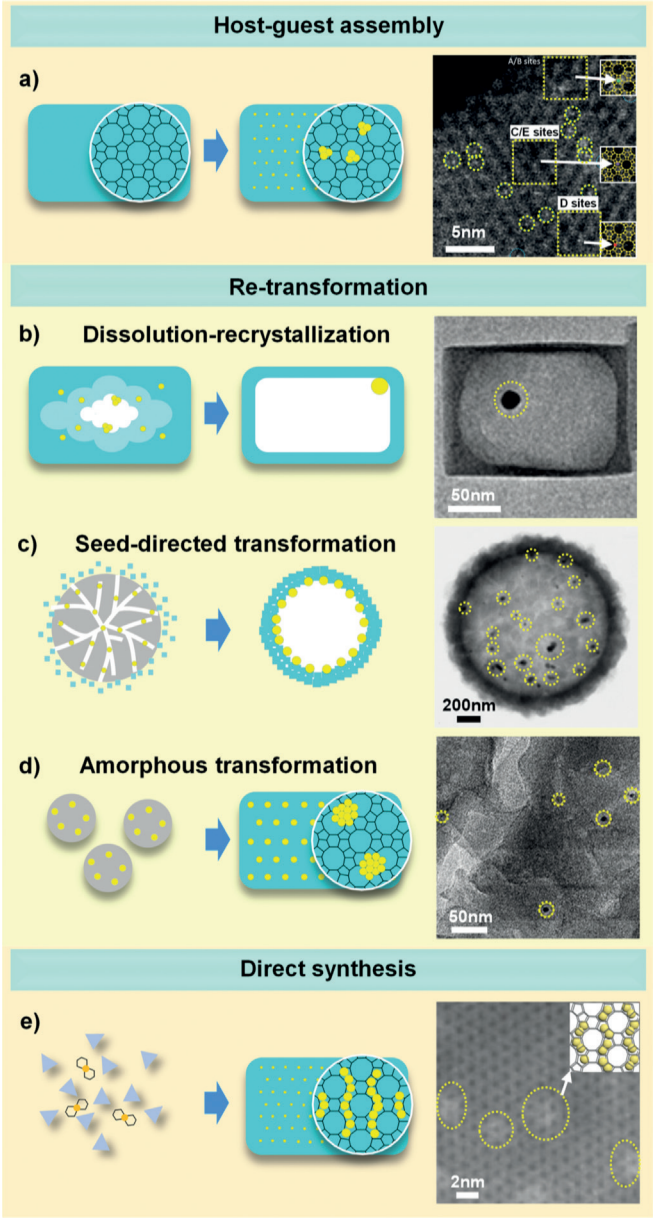

Figure 2. Illustration of the synthesis routes and representative images of different zeolite-confined noble metals. a) STEM image of Pt-oxide/KLTL (Reproduced with permission.[55] Copyright 2014, Wiley.), b) TEM image of Pt@Silicalite-1 (Reproduced with permission.[59] Copyright 2014, American Chemical Society.), c) TEM image of Ag@Silicalite-1 (Reproduced with permission.[50] Copyright 2003, Wiley.), d) TEM image of Pd@Silicalite-1 (Reproduced with permission.[58] Copyright 2016, American Chemical Society.), e) TEM image of Pd@Silicalite-1 (Reproduced with permission.[33] Copyright 2016, American Chemical Society.).

the authors describe as a mixture of oxidized and unoxidized platinum complexes, but do not indicate a defined state.[55]

A noteworthy variant uses volatile and more labile organometallic species, such as $[Rh(CO)_2(acac)]$ and $[Ir(CO)_2(acac)]$, which can be incorporated in acidic zeolites from the gas or liquid phase onto the support.[32,46] The zeolite loading has to be carried out with exclusion of air and water, which react with most organometallic compounds. Decomposition of the organometallic precursors are then carried out with thermal treatment under reduced pressure or in a reducing or inert atmosphere.[29]

Additionally, for zeolites, alkali-metal ion exchange is also an effective way to introduce other metal ions (Figure 2a, left). Note that the exchange capacity strongly depends on the number of Al atoms per unit cell as the frameworks acquire their negative charge by substitution of some Si^{IV} by Al^{III} and this negative charge is usually neutralized by alkali-metal cations.[29] For example, platinum oxide was introduced in zeolite KLTL by reaction with $[Pt(NH_3)_4](NO_3)_2$, followed by oxidation at 633 K. A determination of the nuclearity of the platinum complexes species before oxidation was provided by STEM images (Figure 2a, right), which confirmed the presence of exclusively site-isolated single Pt complexes.[55] The $[Pt(NH_3)_4]^{2+}$ species are precisely located right at the edge of the 12-membered rings, between the two 12-membered rings, and in the center of three 12-membered rings (Figure 2a, right). After oxidation at 633 K, Pt-oxide/KLTL zeolite was obtained. The location of some Pt atoms had changed but they were still site-isolated.[55]

It has to be pointed out that such host–guest assembly including wetness impregnation, gas/liquid diffusion, and ion-exchange strongly depends on the pore sizes, pore volume, and framework properties of the zeolitic supports.[29] For example, the loading amount of metal precursor depends on the pore volume of the support. The pore sizes restrict large precursors from entering zeolites with their constricted pores. Ion-exchange is often used in zeolites with high Al-content but is not a good method in zeolites with low amount of Al.

Moreover, one disadvantage of the direct incorporation approach is that the pores of zeolites are too small for the access of larger molecules and this often leads to blocking of pore channels and metal instability or inhomogeneity at the surface. Therefore, under such direct host–guest assembly, it seems unavoidable to have an uneconomic waste of noble metals and a decrease of noble-metal-based activity owing to the disadvantageous inaccessibility of some of the zeolite-confined noble metal content.

2.2. Re-transformation

In recent years, a series of re-transformation processes such as recrystallization from low-crystalline or semi-crystalline supports, seed-directed transformation from mesoporous supports and re-transformation from amorphous supports were developed for the full encapsulation or redistribution of noble metals.[50,56–58]

An elegant example is the transformation from nanometal-supporting low-crystalline zeolites to nanometal-supporting hollow zeolite by dissolution-recrystallization (Figure 2b, left). First, Silicalite-1 was impregnated with an aqueous solution of $[Pt(NH_3)_4](NO_3)_2$. Then the resulting solid was treated with tetrapropylammonium hydroxide-(TPAOH) for recrystallization and the Pt-complex@Silicalite-1 composite was calcined at 450 °C. At high temperature and high pH values, silicalite species are dissolved from inside the host framework and recrystallize on the outer surface. The $[Pt(NH_3)_4](NO_3)_2$ precursor was reduced under H_2 at 300 °C to yield Pt nanoparticles in the inner cavities of the crystals. This way the low-crystalline zeolitic crystals were transformed into hollow boxes, with controllable cavities, shells, and compositions, from pure Silicalite-1 to aluminosilicate ZSM-5, for the encapsulation of various noble metals such as Pt (Figure 2b, right), Pd, Au, and nanoalloys (including PtPd, PtAg, PdAg, AuAg).[56,59–61]

Mesoporous silica materials are often chosen as excellent nanocarriers to support the noble metal nanoparticles. By zeolite-seed-directed transformation (or re-crystallization), the semi-crystalline and/or amorphous mesoporous silica structure can be transformed to crystalline Silicalite-1 (we note that Silicalite-1 is no aluminosilicate but a representative of pure silica zeolite, that is, made entirely of silica and isotypic to the ZSM-5 zeolite with the MFI framework). The mesoporous silica spheres containing noble metals are used to transform to spherical Silicalite-1 with the introduction of Silicalite-1 seeds (Figure 2c, left), resulting in the encapsulated noble metals inside the hollow centers. This secondary hydrothermal transformation has been successfully used to form Pt, Pd, or Ag-encapsulated hollow Silicalite-1 spheres, respectively, (such as Ag@hollow Silicalite-1, Figure 2c, right) and three-dimensionally ordered macroporous Silicalite-1 monoliths.[50,62,63] Note that the nanoparticles within the supports, be it Silicalite-1 or mesoporous silica, would grow to larger particles, owing to the movement, redistribution, and self-aggregation during the recrystallization under aqueous and vapor conditions. Mostly recently, another seed-directed method was developed for confinement of various noble nanometals (Pd, Pt, Rh, Ag) inside different zeolites (Silicalite-1, Beta, Beta-Fe, MOR) to prevent metal sintering.[64,65] Noble metal nanoparticles were first encapsulated in zeolite seeds and then placed into aluminosilicate or silicalite gels to form a crystalline zeolite sheath around the metal-containing seeds. The key for these syntheses was the use of a mixture of zeolite seeds and noble metal nanoclusters, and the resultant catalysts exhibited extraordinary sinter resistance in high-temperature reactions.

A simple amorphous-transformation method is applied to the synthesis of Pd@Silicalite-1 from mixture of amorphous silica nanoparticles and metal precursor chloropalladic acid.[57] The ease of this work is to ensure the complete integration of Pd nanoparticles inside mesoporous Silicalite-1 nanocrystals rather than on their surface. The polyvinyl pyrrolidone (PVP) is needed to disperse metal precursor into amorphous silica aerogel. The aerogel containing metal precursor is transformed to zeolite nanocrystals in the presence of a limited amount of water, and then Pd@Silicalite-1 is finally obtained by calcination and reduction, respectively. An alternative route is a solvent-free amorphous

transformation developed by Wang and Xiao et al., by which the metal nanoparticles remain always highly dispersed inside the amorphous silica during the re-transformation process from amorphous silica to zeolite.[58,66] This solvent-free re-transformation works with the start of metal nanoparticles encapsulated in amorphous silica, which then form a dry gel after adding a structure directing agent and are finally crystallized in an autoclave at 180 °C over 3 days. Pd@Silicalite-1, which is formed this way from Pd nanoparticles contained in amorphous silica, is a good example of Pd nanoparticles which are well-encapsulated inside a porous crystalline silica framework (Figure 2d).[58]

2.3. Direct Synthesis

In general, the nanometals supported in zeolites by host–guest assembly and re-transformation often lead to large and non-uniform nanoparticles as well as unsatisfactory dispersion. A breakthrough of direct synthesis was made to confine the very small nanometals into zeolites using metal ligand-stabilized precursors (so-called ligand-precursors) during the zeolite formation. The ligand-precursors are classical metal coordination complexes, mainly including metal-S complex and metal-N complex (for example, $[Pd(en)_2]^{2+}$ (en = $H_2NCH_2CH_2NH_2$), $[Pt(NH_3)_4]^{2+}$). This method using ligand-precursors takes advantage of the cooperation effect of the organic groups of the metal complex, small organic structure-direction agents, and inorganic zeolite precursors to generate a porous structure.[33] By using these coordination complexes, the precipitation of metal hydroxides in alkaline solution during the zeolite formation could be avoided. A series of uniform and small metal clusters (with for example, Pt, Pd, Ir, Rh, Ag, Au, AuPd, AuPt, PtPd nanoalloys, of sizes between 1 and 3 nm) within different types of aluminosilicates (such as BEA, FAU, SOD, LTA), could be prepared using sufficiently kinetically stable metal complexes under direct hydrothermal zeolite formation conditions.[34,48,49,67–69]

Notably, low-silica zeolites such as BEA and FAU suffer from low hydrothermal stability and weaker Brønsted acidity than Si-rich materials, which limits the applications of low-silica zeolites as catalysts under high temperature conditions. The synthesis of metal nanoparticles encapsulated in high-silica small-pore zeolites or pure silica zeolite such as Silicalite-1 would be therefore of both fundamental and practical interest. $[Pd(en)_2]Cl_2$ was chosen to form small Pd nanoparticles of 1.5 nm diameter encapsulated within nano-sized Silicalite-1 (Figure 2e, left) by a hydrothermal crystallization route followed with calcination and H_2 reduction.[33] The Pd clusters are located within the intersectional channels (Figure 2e, right) and the feature of pure-silica endow the host–guest catalyst system with excellent catalytic activity and stability. This method has been used, so far, for the synthesis of bimetallic nanoalloys (such as PdNi and PdCo) encapsulated in the Silicalite-1 MFI framework with high catalytic activity and stability.[15]

3. Confinement Effects in Confined Catalysis

The superior catalytic properties (see below) and excellent stability of the nano or subnano noble-metal clusters confined in zeolites create new prospects for their practical high-performance catalytic application. Moreover, zeolite-confined noble-metal catalysts encounter challenges during preparation, activation, and operational use for a wide variety of reactions, such as CO oxidation, water-gas shift reaction, selective hydrogenation, deNOx, reforming and other organic reactions (Table 1).

Here, we illustrate confinement effects (including size, encapsulation, recognition and synergy effects) to better understand the advantages and features of confined catalysis, showing excellent activity, stability, and selectivity.

3.1. Size Effect for Activity Enhancing: From Nanoscale to Atomic Sites

In general, noble metal nanoparticles possess unique nanoscale effects and improved catalytic properties compared

Table 1: Catalytic reactions and catalysts of various zeolite-confined noble metals.

Catalytic reactions	Catalysts
CO oxidation ($CO + O_2 \rightarrow CO_2$)	Pt/KLTL,[55] Pt/Silicalite-1,[59] Pt/Beta,[64] Pt/ZSM-5.[70]
Oxidation of hydrocarbons (e.g. $CH_4 + 1/2\,O_2 \rightarrow CO + 2\,H_2$, epoxidation)	Pd/H-ZSM-5,[35] Pt/Silicalite-1, ≈/Beta,[64] PtPd/TS-1,[71] Au/TS-1.[72–74]
Oxidation of alcohols (e.g. $2\,CH_3CH_2OH + O_2 \rightarrow 2\,CH_3CHO + 2\,H_2O$)	Pt, Pd, Rh or Ru/SOD, ≈/GIS, ≈/ANA,[49] Au/Silicalite-1,[51] AuPd, AuPt, PdPt/Na-LTA,[34] Pt, Ag/Silicalite-1.[62]
Water-gas shift ($CO + H_2O \rightarrow CO_2 + H_2$)	Pt/Beta,[64] Au/NaY.[75]
Selective hydrogenation (e.g. alkenes, alcohols and aldehydes)	Pt/MCM-22,[52] Pt/CHA,[54] Pd/Silicalite-1.[76]
Other organic reactions (e.g. coupling reactions, hydrochlorination, hydrofluorination)	Pd/Silicalite-1,[57] Pd/NaY,[77] Pt/H-ZSM-5,[78] PtIr/H-ZSM-5,[79] Pd/HY[80], PtPd/USY[81], PtPd/ZSM-5.[82]
deNOx	Pt/USY,[83] Ir/ZSM-5,[84] Au/ZSM-5,[85] Pt/ZSM-5,[86] Au/NaY, ZSM-5,[87] Pt/Beta.[88]
Reforming reactions (e.g. dehydrogenation, dehydrocyclization, hydroisomerization, hydrocracking)	Pt/ZSM-5[89], Pt/ZSM-22[90], Pt/HZSM-5[91], Pt/USY[92], Pt/ZSM-5, ≈/Beta.[93]

with larger microscale bulk metals because of more exposed active sites per molar amount of metal.[40] In the last decade, the rapid development of the above-mentioned synthesis strategies provides a good chance to understand the unique mechanism and effects of different sizes of nanometals in zeolites. Particle sizes of nanometals in zeolites have been precisely controlled, for example, nanoscale sizes by nano-encapsulation, subnanoscale sizes by traditional impregnation and atomic-scaled sites by framework fixation. As it is well-known, the size decrease generates an increase of unsaturated metal surface atoms; thus the surface free energy of the metal species increases, and more and more metal sites become also active for metal–support interactions.[94–96] Different to other supports, size effects in zeolites can be better understood, because of the precise control of particle sizes in the same type or topological structure of zeolites. That means that size effects of noble metals can be investigated in a very similar support environment. Note that the unique crystal structure of zeolites even affects the sizes of nanometals on a 0.1 nm level, for example by using K^+ instead of Na^+.[33]

The recent studies on nanoscale effects of zeolite-confined nanometals (Figure 3a) show that the deviation of their

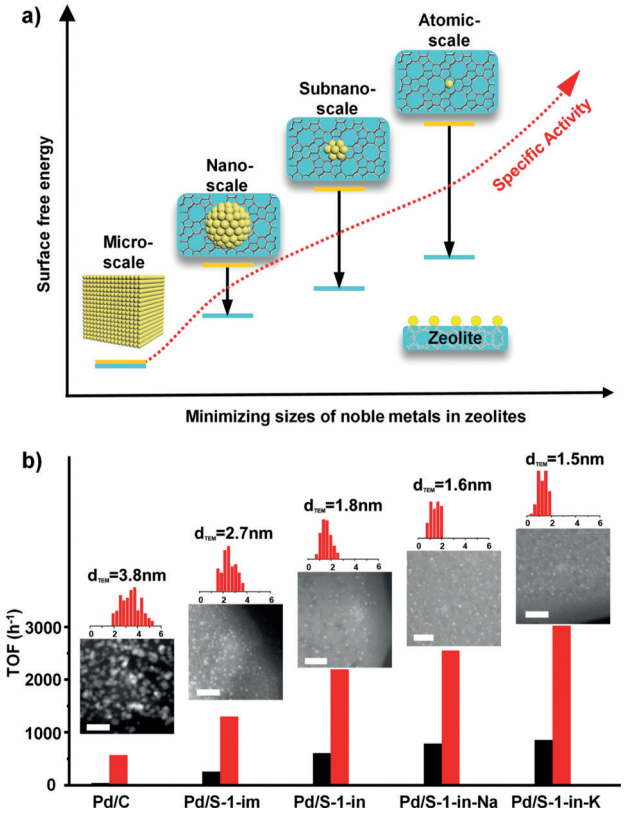

Figure 3. Size effect of noble metals in zeolites. a) Illustration of the changes of surface free energy and specific activity with the size of noble metal particles in the zeolite support; b) TOF values of H_2 generation from the dehydrogenation of formic acid–sodium formate (1:1) at 25 °C (black) and 50 °C (red) with Pd nanoparticles of different average size on either carbon (Pd/C) or in Silicalite-1 (Pd/S-1) (im = impregnation, in = in situ encapsulation). Insets: TEM images and corresponding size distributions of Pd clusters. Scale bars: 20 nm. Reproduced with permission.[33] Copyright 2016, American Chemical Society.

atomic and electronic structures from the expected electronic structure at very small nuclearities might be due to their interaction with the framework.[40,97] The nanometals may be charged as a result of incomplete reduction or of interactions with the framework. The catalytic activity normally increases with the decrease of the particle size. Recent theoretical and experimental studies have demonstrated that subnanometer-sized metal clusters can have a better catalytic activity or selectivity than the nanometer-sized counterparts.[40,98,99]

A unique example of size effect was reported by Yu et al. about well-dispersed and small Pd nanoparticles in nanosized Silicalite-1 (Pd/S-1-in).[33] The size of Pd cluster can be decreased by using alkali hydroxide in the synthesis procedure, because the alkali cations like K^+ and Na^+ may reduce some void spaces of the channels.[33] It was obvious that smaller Pd nanoparticles (1.8 nm in Pd/S-1-in) were obtained, compared with commercial Pd/C (3.8 nm) and Pd/S-1 via impregnation (Pd/S-1-im, 2.5 nm; Figure 3b). While using alkali hydroxide, the size can further decrease to 1.6 nm in Pd/S-1-in-Na and 1.5 nm in Pd/S-1-in-K. In the H_2 generation reaction from the complete decomposition of formic acid, the Pd/S-1-in-K catalyst gave the highest turnover frequency, TOF of 856 h^{-1} at 25 °C and 3027 h^{-1} at 50 °C, which is about 1.1 fold of Pd/S-1-in-Na, 1.4 fold of Pd/S-1-in, 5-fold of Pd/S-1-im, and 19-fold of a Pd/C catalyst at 25 °C (Figure 3b). Notably, under similar conditions, the TOF value of smallest size in this work is not only among the highest activities, but also the size effect could be perfectly defined and possibly investigated as a model for the relationship of size/activity.[33]

Similar size effects have been used in the high-performance design of a nanoscale to atomic distribution of metal species in zeolites.[52,54,55] A remarkable work by Corma et al. was MCM-22-confined subnanometric Pt species (single Pt atom and/or subnano Pt cluster) catalysts.[43] A very small particle size (0.2–0.7 nm) of Pt in Pt@MCM-22 showed an excellent catalytic activity in propylene hydrogenation, which was about five times higher than conventional Pt/MCM-22-im (1–6 nm).

Accordingly, atomically distributed active metal centers could be the ultimate goal of fine dispersion in zeolites. An ideal case may be single atom sites confined in the cages or channels of the frameworks, because of the maximized free energy of metal surface species, which could then lead to unique chemical properties of single atom catalytic centers and maximum utilization of noble metals.

3.2. Encapsulation Effect for Stability Enhancement: From Nanostructured Fixation to Supercage Stabilization

The active atoms of nanometals are generally located at corners and edges, and tend to sinter under harsh reaction conditions.[100,101] As a result of this low thermal stability, noble nanometal deactivation by Ostwald ripening or particle migration and coalescence is a big limitation for their industrial application. Long-term stability and high activity of the nanometals are therefore crucial in their applications. Encapsulation, as an efficient and sustainable solution,[102] has been developed to overcome this problem and to confer high

activity and extended lifetime to nanometal catalysts. Nanostructured core–shell or yolk–shell zeolites are often used to encapsulate the metal nanoparticles (Figure 4a). The noble-metal particles are usually dispersed in the cores and are fixed by the shells, which prevent growth by sintering. Such an encapsulation by nanoscale fixation has been an efficient way to a high-performance catalyst design, for example, for Pt nanoparticles encapsulated in a hollow single-crystal Silicalite-1 catalyst for CO oxidation.[59] While the silicalite shell limits transport of propylene to the metal particles, CO is converted into CO_2 by Pt nanoparticles. The unique yolk-shell structure shows a remarkable resistance to poisoning by propylene during CO oxidation.

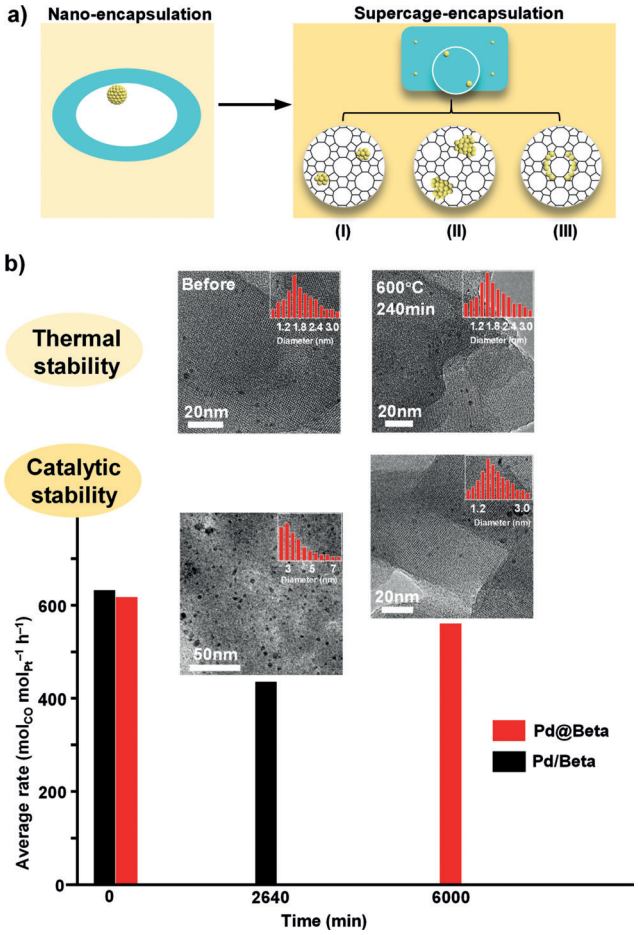

Figure 4. a) Model of the location of noble metal nanoparticles and nanoclusters in zeolites. b) The HRTEM tomographic images and size distributions of nanoparticles of Pd@Beta and Pt@Beta after calcination at 600 °C for 240 min; average rate of Pd@Beta and Pd/Beta in the water-gas shift reaction at 300 °C and the corresponding TEM images of Pd@Beta and Pd/Beta after the water-gas shift reaction. Reproduced with permission.[64] Copyright 2018, Springer.

Strong interactions between the noble metals and zeolites are mostly preferred for stabilizing the nanometals. The unique supercages of zeolites offer a strong electrostatic interaction and limited spatial volume to change the electronic configuration of nanometals, which allow for the kinetic stabilization of thermodynamically unstable metal clusters. Noble metals encapsulated in the supercages of zeolites can be summarized into the three categories (Figure 4a): I) in the zeolite micropores, II) inside of the zeolite crystals, and III) in the intersectional void spaces.

Zeolite frameworks in which pores delimit relatively large cavities interconnected to each other by subnanometric windows are particularly interesting. Therefore, in early studies, clusters were formed inside those cavities. These clusters were generally too large to escape from the cavities and thus showed very high stability.[103–105] An innovative way was developed by Wang and Xiao's group to a series of noble-metal@zeolite catalyst in the widely useful size range of 0.8–3.6 nm, even larger than zeolite channels.[64] The size of Pd nanoparticles in a Pd@Beta catalyst were well maintained after the high-temperature treatment at 600 °C (Figure 4b, top), which indicated their extraordinary sinter resistance. Besides, in long-time water-gas shift reactions, the Pd@Beta catalyst maintained more than 90% activity (from 615 $mol_{CO}\,mol_{Pt}^{-1}\,h^{-1}$ to 561 $mol_{CO}\,mol_{Pt}^{-1}\,h^{-1}$) after 6000 min while the activity of conventional supported Pd/Beta by impregnation decreased 30% (from 630 $mol_{CO}\,mol_{Pt}^{-1}\,h^{-1}$ to 435 $mol_{CO}\,mol_{Pt}^{-1}\,h^{-1}$) after 2640 min. (Figure 4b, middle and bottom). Note that after usage, the Pt@Beta catalyst still incorporated platinum nanoparticles in the original diameter range of 0.8–3.2 nm, whereas after its use, Pt/Beta incorporated much larger nanoparticles (2–8 nm) than before (1.2–3.3 nm).[64]

Most importantly, these entrapped noble-metal clusters have been expanded to many catalysis reactions such as a series of metal@zeolite (including Pt@Beta, Pt@MOR, Rh@Beta, Rh@MOR, Ag@Beta, Ag@MOR) for CO oxidation, oxidative reforming of methane and the water-gas shift reaction,[64] Pd@Beta for hydrogenation of nitroarenes,[65] and Pd@Silicalite-1 for C–C coupling reactions,[57] where they exhibit high activity and good shape selectivity, as well as excellent stability (such as a remaining yield of 93% after 15 runs in C–C coupling reactions).[57]

The key effect of encapsulation is to significantly improve the stability of zeolite-confined noble metals and the resultant catalysts exhibit extraordinary sinter resistance, especially in the high-temperature reactions.

3.3. Recognition Effect for Selectivity Enhancement: From Molecular Sieve to Site Adsorption

Nature makes abundant use of high selectivity, especially in that enzymes usually process only very few molecules which fit into their active sites. For zeolite-based catalysis, shape selectivity (so-called molecular sieving) means that the transformation of reactants into products depends on how the processed molecules fit into the pores of the zeolite and then to the active sites of the catalyst. For zeolite supports, the shape or topology of the porous structures can strongly affect the selectivity on the molecular level. Industry has also exploited shape selectivity in zeolite catalysis for almost 50 years.[106–108] For research on zeolite-confined catalysts it is in reversal important to show a shape selectivity of the zeolite-catalyst system to prove that the catalysis does indeed

take place inside the zeolite pores and not only on catalysts which are attached to the outer surface or at pore mouths.

In early studies and in the traditional definition, shape selectivity often refers to reactants, intermediates, and products. In a catalytic reaction the substrate molecule first enters into an interaction with the active site of the catalyst; intermediates may form, which then convert into the final product, which leaves the catalyst site. Therefore, once the mass transfer of reactant or product is limited, a low conversion would occur. Such a limitation of mass transfer can derive from the shapes, sizes, and topologies of reactants, intermediates, and products in connection to the zeolite support framework. In other words, if any reactant in a feed mixture cannot diffuse into the zeolite framework, these reactants will remain unreacted and end up in a mixture with the products (Figure 5a). A recent work discovered that the relative fast diffusion directly affects the selectivity and conversion.[54] For example, when chabazite supported Pt species in Pt@CHA were tested in the hydrogenation of olefins of different sizes, more than 80% ethylene (0.39 Å) but no propylene (0.45 Å) were converted under identical conditions, because the permeation of ethylene was faster than propylene.[54]

With further understanding of the mechanism, it was realized that transition-state selectivity can occur. The topologies of zeolites strongly influence the rates of adsorption and reaction by the adjustment of relative Gibbs free energies of the transition states.[109,110] Similar to the shape selectivity of reactants, the more bulky transition states do not form inside the pores of zeolites, and the reaction intermediates cannot continue to undergo consecutive reactions.[109,111]

The shape-sieve property of zeolite supports has been thoroughly investigated by testing the molecule-size dependent selectivity of Pd nanoparticles inside Silicalite-1 (Pd@S-1) nanocrystals in the reaction of molecules with different sizes.[57] In the hydrogenation of nitrobenzene and 1-nitronaphthalene, the yield of aniline can reach up to 94% while only a negligible amount of 1-nitronaphthalene was converted into 1-aminonaphthalene in Pd@S-1, because 1-nitronaphthalene with a large molecule size (7.3×6.6 Å^2) could not pass through the micropores (pore size: 5.3×5.6 Å^2) of Silicalite-1 (Figure 5b). At the same time the size-dependent selectivity results of Pd@S-1 demonstrated that the hydrogenation of nitroarenes took place inside the pore system. A similar size/shape selectivity of Pd@S-1 was also observed in oxidation and carbon–carbon coupling reactions.[57]

Apart from the shape selectivity enacted by the pore size of the zeolite support, the adsorption state of reactants on the catalyst site also influences the catalytic selectivity and activity.[112,113] The site adsorption on the metal surface is therefore also critical after the pore selectivity. Recent work by Xiao's group used a Pd@Beta catalyst with high selectivity in the hydrogenation of substituted nitroarenes.[65] While the zeolite micropores determine the steric arrangement of the molecules into the pore channels, the Pd sites fixed in the zeolite have a selective adsorption to different organic groups. The adsorption of 4-nitrochlorobenzene to the Pd sites, occurs primarily via the nitro rather than the chloro group owing to the stronger interaction of the nitro group with the Pd surface

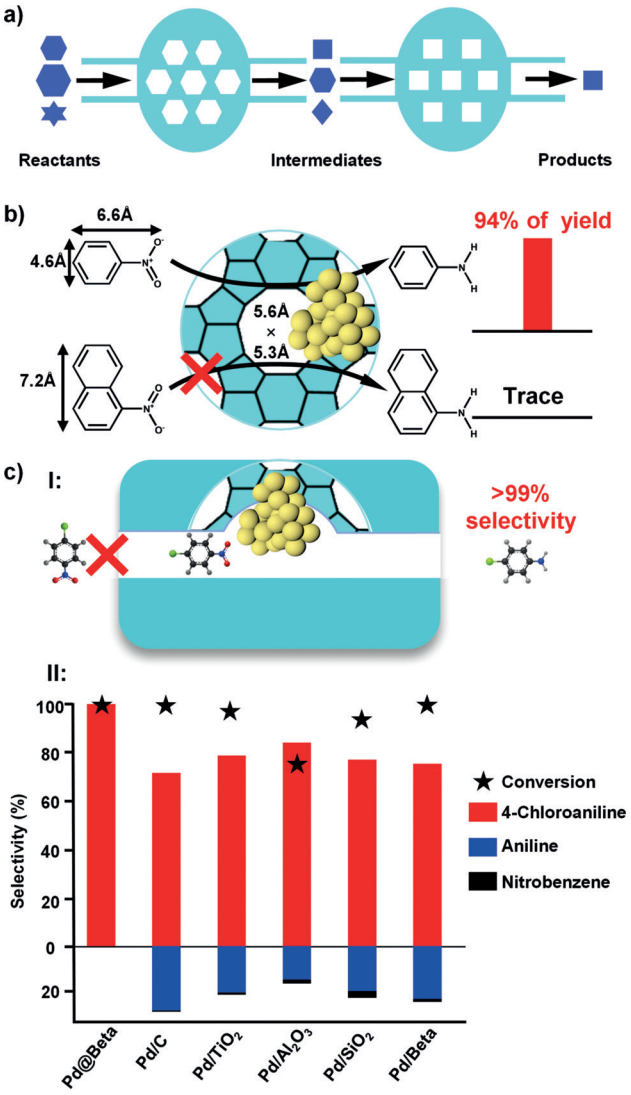

Figure 5. a) Illustration of the shapes, sizes, and topology selectivities of a zeolite support. b) The size-selective catalysis of Pd@S-1 in the hydrogenation of nitroarenes. Reproduced with permission.[57] Copyright 2016, Wiley. c) Selectivity of Pd@Beta. I: The proposed models for the adsorption of 4-nitrochlorobenzene on Pd@Beta. II: Substrate conversions (star) and product selectivities (colored columns and numerical *y*-axis values) for the hydrogenation of 4-nitrochlorobenzene on various catalysts. Reproduced with permission.[65] Copyright 2017, Wiley.

(Figure 5c, I). Subsequently, in the conversion of 4-nitrochlorobenzene, Pd@Beta showed a selectivity greater than 99.0% of 4-chloroaniline, while on conventional supported Pd catalysts (Pd/C, Pd/TiO_2, Pd/Al_2O_3, and Pd/SiO_2), dechlorination occurs with 4-chloroaniline selectivities ranging from 70.9% to 89.6% (Figure 5c, II). The extraordinary selectivity of Pd@Beta was attributed to the sterically selective adsorption and was further confirmed by competitive adsorption and adsorbate displacement tests.[65]

The expected shape selectivity of zeolites is important for a catalytic selectivity because the steric restrictions offered by the pores, caves and cages limit the sizes and diffusion of reactants and products and influence the transition state or

which species can enter and leave the active sites. The selective adsorption at confined metal sites is another possibility to induce a selective catalytic reaction, in comparison with only shape-selective ones.[52]

3.4. Synergy Effect for Multifunctional Design: From Dual Sites to Cascade Reactions

Zeolites can provide a specific platform for nanometals, for example, protective microenvironments and functional sites for catalytic reactions. For example, combined with noble metal sites, acidic zeolites enable dual-site catalysts capable of catalyzing different types of reactions on dual active metal and acid sites (Figure 6a, inset).[114–116] Dual-site catalysts usually have unique properties due to the synergy between metals and acidic functions.[117] Generally, in a catalytic reaction, the confined noble metal in the acidic zeolite will strongly influence the state of the acid sites. For example, Pt and Ir metal nanoparticles became involved in charge transfer with neighboring framework atoms of Beta and Y zeolites and thus affected the mean framework electronegativity of the zeolites as was shown by ^{1}H magic-angle spinning (MAS) NMR and FTIR spectroscopy.[118] At the same time, the zeolite framework will have a confinement effect to the electronic structure and coordination state of surface atom sites of noble metal clusters.[35] Therefore, bifunctional catalysts could show advantageous synergistic effects in reducing the energy compared with the independent functions of acid sites and noble metal sites (Figure 6a).[114]

To better understand the bifunctionality of MFI-type zeolites with supported Pd nanoparticles, the hydroconversion of furfural (FFL), as a model reaction, has been investigated.[117] Remarkably, different products were obtained when the zeolite support changed from Silicalite-1 over Na-ZSM-5 to H-ZSM-5, respectively. Temperature-programmed desorption studies reveal that both the adsorption of furfural and the activation of H_2 on encapsulated palladium species are significantly affected by the zeolite microenvironment, which accordingly led to different pathways in the furfural hydroconversion catalyzed by the Pd@MFI networks of S-1, Na-ZSM-5, and H-ZSM-5 (Figure 6b). The additional functionalities provided by the ZSM-5 zeolites were investigated by means of temperature-programmed desorption (TPD) of NH_3, H_2 and furfural probe molecules (Figure 6b). The NH_3-TPD showed a clear signal for Pd@H-ZSM-5, indicating and quantifying the abundant acid sites that are available for Brønsted acid catalytic activities. In H_2 adsorption, higher amount of H_2 are adsorbed on both Pd@Na-ZSM-5 and Pd@H-ZSM-5 than on Pd@S-1, indicating a promotion effect for H_2 adsorption of the zeolite frameworks and their aluminum content over an all-silicon framework like Silicalite-1, which just has the same MFI structure. The desorption of FFL shows slight differences between Pd@S-1 and Pd@H-ZSM-5 and the desorption temperature increases with more acid sites. In the hydroconversion of furfural, the main product by Pd@H-ZSM-5 was 1,5-pentanediol by hydrogenolysis–hydrogenation (Figure 6b).[117]

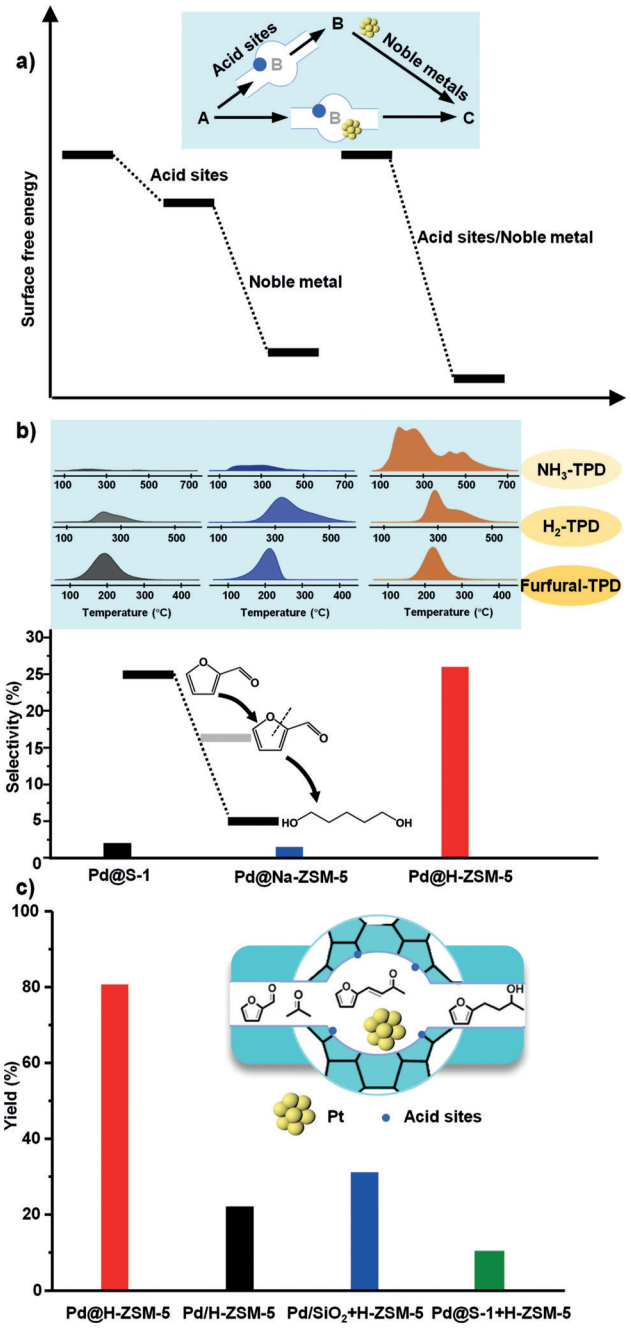

Figure 6. a) Illustration of the possible bifunctionality and synergistic effect by the catalyst with both acid sites and noble metal active sites. Inset: model of a cascade reaction by the bifunctional catalyst. b) The selectivity of different catalysts in the hydroconversion of furfural into 1,5-pentanediole. Inset: NH_3-TPD, H_2-TPD, and furfural-TPD of Pd@S-1 (black), Pd@Na-ZSM-5 (blue), and Pd-H-ZSM-5 (red). Reproduced with permission.[117] Copyright 2018, American Chemical Society. c) Yields of combined 4-(2-furyl)butan-2-ol (FAc-HH) and 4-(2-furyl)butan-2-one (FAc-H) for sequential aldol addition, condensation and hydrogenation of furfural with acetone over the tested catalysts. Thereby the yield of the minor condensation product FAc-H is only 3.2%, 8.2%, 8.5%, and 5.9% for the four catalysts. Inset: illustration for the consecutive reactions to fully-hydrogenated FAc-HH. Reproduced with permission.[36] Copyright 2018, American Chemical Society.

A similar synergistic effect also guides the CH_4 combustion over Pd/H-ZSM-5 catalysts, which show high performance at low temperature.[35] The interactions between the surface Brønsted acid sites of H-ZSM-5 and the Pd oxide species, that is, the relationships between the synthesis conditions and electronic structures of Pd oxide were investigated experimentally and theoretically. The theoretical and experimental evidence show that the Pd oxide species anchored by Brønsted acid sites of H-ZSM-5 exhibit strong Lewis acidity and lower oxidation states, which is beneficial to the C–H bond activation and corresponding reduction of the reaction barrier.[35]

Further, multifunctional catalysts inspired by bifunctional catalysts would be possible to achieve multistep cascade reactions (also called tandem reactions) in one pot. Such reactions are extremely important for sustainable synthesis with lower cost, fewer chemicals, and less energy consumption. It enables multiple reactions to occur in a single system and at similar conditions, which is considered as a promising and valuable process for decreasing the cost of separation steps and increasing energy utilization efficiency.[119,120] Generally, dual or more kinds of active sites are needed in cascade reactions to ensure the catalysis of each step. Further, it is of great importance to precisely control the distribution of different active sites for selectively driving specific cascade reactions.[121]

Recently, a Pt@H-ZSM-5 metal-acid catalyst has been used in a one-pot cascade catalytic reaction.[36] The cascade reaction is the aldol condensation of furfural with acetone and the subsequent hydrogenation of the adduct over Pt@H-ZSM-5, with the hydrogenated aldol adduct as the target product (Figure 6c, inset). As a result, a combined yield of 81% for the hydrogenated aldol adducts 4-(2-furyl)-butan-2-one (FAc-H, 3%) and 4-(2-furyl)butan-2-ol FAc-HH (78%) was achieved on Pt@H-ZSM-5 (Figure 6c). In contrast, a much lower yield toward the cascade reaction were exhibited in Pt/H-ZSM-5 (22%), physically mixed Pt/SiO_2 and H-ZSM-5 (27%) and physically mixed Pt@S-1 and H-ZSM-5 (10%). The significantly distinct yields are attributed to the distribution of metal and acid sites. If Pt nanoparticles would have been on the external surface, it would have led to efficient furfural conversion into furfuryl alcohol as the main product by Pt-catalyzed hydrogenation before the aldol condensation by the acid sites at the internal surface of the zeolite. Therefore, for Pt nanoparticles encapsulated in Pt@H-ZSM-5, the zeolite host will limit the access of furfural to the Pt sites, leading to the preferential conversion of furfural via the aldol condensation pathway.[36]

Multifunctional metal-supported catalysts (Pt/H-ZSM-5 and Pd/H-ZSM-5) for glycerol to hydrocarbon conversion have been investigated by Varma et al.[122] The multistep reaction starts with the deoxygenation of glycerol to oxygenates and other intermediates such as short-chain hydrocarbons (both paraffins and olefins) and/or monohydric alcohols. Then, aromatic species are generated by combining short-chain species in the channel or on the acidic sites of H-ZSM-5 zeolite. With the enhancement of the aromatic yield by Pd nanoparticles, around 90% glycerol conversion and 60% yield of aromatic hydrocarbons were achieved over the Pd/H-ZSM-5 catalyst. It provides a new perspective on the conversion of glycerol into hydrocarbon by designing a bifunctional catalyst.[122]

As a highlight of multifunctional catalysts, the cascade reactions, which depend on and use synergy effects are a sequential transformation of reactants with immediate utilization of intermediates to lead to the formation of products without separation steps. The cascade reactions thus offer great advantages with respect to economizing on costs and time, and limit undesired mass or energy losses.[123]

4. Challenges and Opportunities

Rapid progress in the zeolite-confined noble metals has taken place in the last few years, with the opportunities presented by the successes in confined catalysis. However, much remains to be learned. The states and reactivities of supported metal clusters are still not well known, although much progress have been made to investigate the above-mentioned problems of unknown states and reactivities of supported metal clusters. The effects of zeolites on metal cluster structure and the nature of the metal-zeolite interface are less than well understood.[41,42,99] Theoretical chemistry is beginning to have an impact on the assessment of electronic properties, with calculations having been reported,[45,124] but it is still too early for theories to account reliably for the influence of the support.

The important opportunities and challenges in catalysis are a precise design on the combination of both metals and zeolites to the reactions for which the activity or selectivity of multifunctional confined catalysts is superior to the conventional current commercial catalysts. The following goals are essential to address in order to push forward the confined-catalysis applications.

1) Practical demand of the noble metals: The high cost in noble metal-based catalysts is still one of the major challenges which can hinder their further large-scale application even if the noble metals are widely used in practical industrial procedures. Non-noble metals such as transition metals could be a possible alternative,[125] however their often low activity, selectivity, and stability still need to be addressed. It is therefore an emerging demand to maximize the activity of heterogeneous noble-metal catalysts and minimize their losses by engineering suitable composites, morphologies, and structures. Significant progress has been recently made in single atom catalysts, which can enable the reasonable use of metal resources and facilitate atom economy.[6] The catalytic activities of atom catalysts can be greatly enhanced by maximizing the expression of active sites toward a specific reaction. However, achieving single atom distributions in zeolites still face many difficulties because of uncontrolled aluminum sites, low supercage specificity or framework differentiation, and low level defects.[32,42] Until now, there is no example showing the feasibility of single-atom catalysis in zeolites, although atomic sites or single metal complexes have been suggested in a few works, albeit

apparently without definitive evidence on the exact species state.[55]

2) Hierarchical control of the zeolite structures: The limitation of matter diffusion in microporous systems is a main problem for industrial catalysis. Hierarchically porous structures could provide zeolite-confined nanometal catalysts with a perfect combination of porosity and nanoscale,[16,17] which not only decrease the loading amount of noble metals but also increase their utilization efficiency owing to their high surface area, rich edge/corner atoms, and the synergetic effect. Ideally hierarchical porous supports have both well-defined macropores and interconnected mesopores involving tunable microporous and mesoporous nanoscale units. More importantly, on all length scales, the larger pores should be connected to the smaller pores, where reactants and products are able to enter and exit, respectively, the interconnected mesopores.[126] Well-defined macroporous structures can significantly improve the active site accessibility. In comparison, industrial catalysts often only mix micro-, meso-, and macro-pores, showing no hierarchy but disordering. Therefore, the control of hierarchical zeolite structures will be a favorable choice.
3) Emerging need of catalysis applications: A key objective of industrial catalysis research are cascade reactions as an effective process of eliminating costly separation steps and increasing energy efficiency. Multifunctional catalysts are therefore in great demand. Zeolite-confined noble metals, which have both active centers of the noble metal guest and the zeolite host, are interesting to achieve cascade reactions. However, there are only a few successes.[36] One problem is the exposure of reactants to both active sites, which might make the reactions occur in parallel instead of in a specific order. Therefore, tailoring the distribution of different active sites is essential in the multifunctional catalyst design. The spatially compartmentalized hierarchical structure may be a rational design.[127] Considering the limitation of zeolite pores, the uncertainty of sites and the difficult size control of noble metals, zeolite-confined noble-metal catalysts with concise and designable acid sites and noble metal sites for cascade reactions still have a long way to go.
4) Future requirement of mechanism extension: Confinement effects are the most important features of zeolite-confined noble-metal catalysts. These catalysts are mostly used in thermocatalytic reactions, such as oxidation, hydrogeneration, and so on.[57,65] At the same time, good examples also exist in the applications of electrocatalysis (such as methanol oxidation), photocatalysis (photodegradation of volatile organic compounds, VOCs), and biocatalysis (enzyme catalysis).[128–130] However, in other specific catalysis types such as enantioselective chiral catalysis, the presented metal@zeolite systems are still very difficult to be used owing to their lack of chiral features and recognition, but it would be an important future aspect.

Note that the defined structures of zeolites give rise to confinement effects such as high size and shape selectivity, and such defined structures are not found in other traditional porous supports such as carbons, silica or metal oxides and organic polymers. It could therefore be of scientific interest and technological importance to extent unique mechanism and effects of zeolites to other supports. Recently, zeolite-related metal–organic frameworks (MOFs) also show similar confinement effects due to their well-defined pore structure. MOFs supplement zeolites with their organic–inorganic hybrid nature, controllable modularity, tunable porosity, and possible implementation of chirality. MOF-confined noble metals are also developing rapidly, not only as multifunctional catalysts.[131] The range of nanoparticles@MOFs is even more extensive with potential applications investigated in molecular adsorption and separation, catalysis, sensing, optics, sequestration of pollutants, drug delivery, and renewable energy, as covered by recent reviews.[131] Further, the appropriate size control of noble metals, the specific selection of support and the precise tailoring of active sites are crucial for the development of confined catalysis.[40,132]

Although zeolite-confined noble metals have been studied in industry for almost 50 years, it is still at the beginning and needs further and deeper investigation in many aspects such as electrocatalysis, photocatalysis, and in commercial applications. Much remains to be learned about the structures, reactivities, and catalytic properties of these materials. Advancement of this understanding will require continued developments in characterization science and extension of synthetic methods to broaden the class of materials. In view of the recent advances in zeolites-confined noble metals and their applications it appears that the future in this research area is bright.

Acknowledgements

We acknowledge a joint DFG-NSFC project (DFG JA466/39-1, NSFC grant 51861135313). This work was also supported by NSFC [U1662134, 51472190, 51611530672, 21711530705], the National Key R&D Program of China [2017YFC1103800], HPNSF [2016CFA033], the Open Project Program of State Key Laboratory of Petroleum Pollution Control [Grant No. PPC2016007] and the CNPC Research Institute of Safety and Environmental Technology.

Conflict of interest

The authors declare no conflict of interest.

How to cite: *Angew. Chem. Int. Ed.* **2019**, *58*, 12340–12354
Angew. Chem. **2019**, *131*, 12468–12482

[1] P. K. Jain, X. Huang, I. H. El-Sayed, M. A. El-Sayed, *Acc. Chem. Res.* **2008**, *41*, 1578–1586.
[2] I. Chakraborty, T. Pradeep, *Chem. Rev.* **2017**, *117*, 8208–8271.
[3] T. K. Sau, A. L. Rogach, F. Jäckel, T. A. Klar, J. Feldmann, *Adv. Mater.* **2010**, *22*, 1805–1825.
[4] S. Guo, E. Wang, *Nano Today* **2011**, *6*, 240–264.

[5] W. Liu, A. K. Herrmann, N. Bigall, P. Rodriguez, D. Wen, M. Oezaslan, T. Schmidt, N. Gaponik, A. Eychmüller, *Acc. Chem. Res.* **2015**, *48*, 154 – 162.
[6] X. F. Yang, A. Wang, B. Qiao, J. Li, J. Liu, T. Zhang, *Acc. Chem. Res.* **2013**, *46*, 1740 – 1748.
[7] A. Wang, J. Li, T. Zhang, *Nat. Rev. Chem.* **2018**, *2*, 65 – 81.
[8] B. Qiao, A. Wang, X. Yang, L. F. Allard, Z. Jiang, Y. Cui, J. Liu, J. Li, T. Zhang, *Nat. Chem.* **2011**, *3*, 634 – 641.
[9] H. J. Sang, J. Y. Park, C. K. Tsung, Y. Yamada, P. Yang, G. A. Somorjai, *Nat. Mater.* **2009**, *8*, 126 – 131.
[10] J. Ying, X. Y. Yang, Z. Y. Hu, S. C. Mu, C. Janiak, W. Geng, M. Pan, X. Ke, G. V. Tendeloo, B. L. Su, *Nano Energy* **2014**, *8*, 214 – 222.
[11] J. Ying, C. Janiak, Y. X. Xiao, H. Wei, X. Y. Yang, B. L. Su, *Chem. Asian J.* **2018**, *13*, 31 – 34.
[12] R. Li, K. Bian, Y. Wang, H. Xu, J. A. Hollingsworth, T. Hanrath, J. Fang, Z. Wang, *Nano Lett.* **2015**, *15*, 6254 – 6260.
[13] H. Song, F. Kim, S. Connor, G. A. Somorjai, P. Yang, *J. Phys. Chem. B* **2005**, *109*, 188 – 193.
[14] Y. Lu, X. Cheng, G. Tian, H. Zhao, L. He, J. Hu, S. M. Wu, Y. Dong, G. G. Chang, S. Lenaerts, S. Siffert, G. Van Tendeloo, Z. F. Li, L. L. Xu, X. Y. Yang, B. L. Su, *Nano Energy* **2018**, *47*, 8 – 17.
[15] Q. Sun, N. Wang, Q. Bing, R. Si, J. Liu, R. Bai, P. Zhang, M. Jia, J. Yu, *Chem* **2017**, *3*, 477 – 493.
[16] a) X. Y. Yang, L. H. Chen, Y. Li, J. C. Rooke, C. Sanchez, B. L. Su, *Chem. Soc. Rev.* **2017**, *46*, 481 – 558; b) M. H. Sun, S. Z. Huang, L. H. Chen, Y. Li, X. Y. Yang, Z. Y. Yuan, B. L. Su, *Chem. Soc. Rev.* **2016**, *45*, 3479 – 3563; c) X. Y. Yang, Y. Li, A. Lemaire, J. G. Yu, B. L. Su, *Pure Appl. Chem.* **2009**, *81*, 2265 – 2307; d) S. M. Wu, N. Jiang, Z. Y. Hu, T. Yan, J. Jin, W. Geng, X. Y. Yang, *Chem. Phys. Lett.* **2019**, *717*, 29 – 33.
[17] W. Schwieger, A. G. Machoke, T. Weissenberger, A. Inayat, T. Selvam, M. Klumpp, A. Inayat, *Chem. Soc. Rev.* **2016**, *45*, 3353 – 3376.
[18] H. Wei, Z. Y. Hu, Y. X. Xiao, G. Tian, J. Ying, G. T. Van, C. Janiak, X. Y. Yang, B. L. Su, *Chem. Asian J.* **2018**, *13*, 1119 – 1123.
[19] H. Huang, X. Wang, *J. Mater. Chem. A* **2014**, *2*, 6266 – 6291.
[20] E. Yoo, T. Okata, T. Akita, M. Kohyama, J. Nakamura, I. Honma, *Nano Lett.* **2009**, *9*, 2255 – 2259.
[21] O. A. Raitman, E. Katz, A. F. Bückmann, I. Willner, *J. Am. Chem. Soc.* **2002**, *124*, 6487 – 6496.
[22] I. Willner, R. Baron, B. Willner, *Adv. Mater.* **2006**, *18*, 1109 – 1120.
[23] W. E. Kaden, T. Wu, W. A. Kunkel, S. L. Anderson, *Science* **2009**, *326*, 826 – 829.
[24] R. J. White, R. Luque, V. L. Budarin, J. H. Clark, D. J. Macquarrie, *Chem. Soc. Rev.* **2009**, *38*, 481 – 494.
[25] J. M. Campelo, D. Luna, R. Luque, J. M. Marinas, A. A. Romero, *ChemSusChem* **2009**, *2*, 18 – 45.
[26] S. M. Wu, X. L. Liu, X. L. Lian, G. Tian, C. Janiak, Y. X. Zhang, Y. Lu, H. Z. Yu, J. Hu, H. Wei, H. Zhao, G. G. Chang, G. Van Tendeloo, L. Y. Wang, X. Y. Yang, B. L. Su, *Adv. Mater.* **2018**, *30*, 1802173.
[27] E. Wahlström, N. Lopez, R. Schaub, P. Thostrup, A. Rønnau, C. Africh, E. Lægsgaard, J. K. Nørskov, F. Besenbacher, *Phys. Rev. Lett.* **2003**, *90*, 026101.
[28] X. Pan, Y. J. Xu, *J. Phys. Chem. C* **2013**, *117*, 17996 – 18005.
[29] P. Gallezot, *Preparation of Metal Clusters in Zeolites*, Springer, Berlin, Heidelberg, **2002**, p. 257.
[30] X. Y. Yang, A. Vantomme, A. Lemaire, F. S. Xiao, B. L. Su, *Adv. Mater.* **2006**, *18*, 2117 – 2122.
[31] X. Y. Yang, A. Vantomme, F. S. Xiao, B. L. Su, *Catal. Today* **2007**, *128*, 123 – 128.
[32] B. C. Gates, *Chem. Rev.* **1995**, *95*, 511 – 522.
[33] N. Wang, Q. Sun, R. Bai, X. Li, G. Guo, J. Yu, *J. Am. Chem. Soc.* **2016**, *138*, 7484 – 7487.
[34] T. Otto, J. M. Ramallo-López, L. J. Giovanetti, F. G. Requejo, S. I. Zones, E. Iglesia, *J. Catal.* **2016**, *342*, 125 – 137.
[35] Y. Lou, J. Ma, W. Hu, Q. Dai, L. Wang, W. Zhan, Y. Guo, X. M. Cao, Y. Guo, P. Hu, G. Lu, *ACS Catal.* **2016**, *6*, 8127 – 8139.
[36] H. J. Cho, D. Kim, J. Li, D. Su, B. Xu, *J. Am. Chem. Soc.* **2018**, *140*, 13514 – 13520.
[37] J. Li, T. Zhao, T. Chen, Y. Liu, C. N. Ong, J. Xie, *Nanoscale* **2015**, *7*, 7502 – 7519.
[38] L. Bui, H. Luo, W. R. Gunther, Y. Román-Leshkov, *Angew. Chem. Int. Ed.* **2013**, *52*, 8022 – 8025; *Angew. Chem.* **2013**, *125*, 8180 – 8183.
[39] a) M. C. Kerby, T. F. D. Jr, D. O. Marler, J. S. Beck, *Catal. Today* **2005**, *104*, 55 – 63; b) A. W. Petrov, D. Ferri, F. Krumeich, M. Nachtegaal, J. A. van Bokhoven, O. Kröcher, *Nat. Commun.* **2018**, *9*, 2545; c) Y. Peng, L. Zhang, Y. Jiang, S. Han, Q. Zhu, X. Meng, F. S. Xiao, *Catal. Today* **2019**, https://doi.org/10.1016/j.cattod.2018.05.032.
[40] L. Liu, A. Corma, *Chem. Rev.* **2018**, *118*, 4981 – 5079.
[41] D. Farrusseng, A. Tuel, *New J. Chem.* **2016**, *40*, 3933 – 3949.
[42] L. Wang, S. Xu, S. He, F. S. Xiao, *Nano Today* **2018**, *20*, 74 – 83.
[43] P. B. Weisz, V. J. Frilette, R. W. Maatman, E. B. Mower, *J. Catal.* **1962**, *1*, 307 – 312.
[44] N. Herron, *Inorg. Chem.* **1986**, *25*, 4714 – 4717.
[45] S. Kawi, J. R. Chang, B. C. Gates, *J. Am. Chem. Soc.* **1993**, *115*, 4830 – 4843.
[46] Z. Xu, F. S. Xiao, S. K. Purnell, O. Alexeev, S. Kawi, S. E. Deutsch, B. C. Gates, *Nature* **1994**, *372*, 346 – 348.
[47] J. Weitkamp, *Solid State Ionics* **2000**, *131*, 175 – 188.
[48] S. Goel, S. I. Zones, E. Iglesia, *J. Am. Chem. Soc.* **2014**, *136*, 15280 – 15290.
[49] S. Goel, Z. Wu, S. I. Zones, E. Iglesia, *J. Am. Chem. Soc.* **2012**, *134*, 17688 – 17695.
[50] A. Dong, N. Ren, W. Yang, Y. Wang, Y. Zhang, D. Wang, J. Hu, Z. Gao, Y. Tang, *Adv. Funct. Mater.* **2003**, *13*, 943 – 948.
[51] A. B. Laursen, K. T. Højholt, L. F. Lundegaard, S. B. Simonsen, S. Helveg, F. Schüth, M. Paul, J. D. Grunwaldt, S. Kegnæs, C. H. Christensen, *Angew. Chem. Int. Ed.* **2010**, *49*, 3504 – 3507; *Angew. Chem.* **2010**, *122*, 3582 – 3585.
[52] L. Liu, U. Díaz, R. Arenal, G. Agostini, P. Concepción, A. Corma, *Nat. Mater.* **2017**, *16*, 132 – 138.
[53] L. Guczi, I. Kiricsi, *Appl. Catal. A* **1999**, *186*, 375 – 394.
[54] M. Moliner, J. E. Gabay, C. E. Kliewer, R. T. Carr, J. Guzman, G. L. Casty, P. Serna, A. Corma, *J. Am. Chem. Soc.* **2016**, *138*, 15743 – 15750.
[55] J. D. Kistler, N. Chotigkrai, P. Xu, B. Enderle, P. Praserthdam, C. Y. Chen, N. D. Browning, B. C. Gates, *Angew. Chem. Int. Ed.* **2014**, *53*, 8904 – 8907; *Angew. Chem.* **2014**, *126*, 9050 – 9053.
[56] S. Li, L. Burel, C. Aquino, A. Tuel, F. Morfin, J. L. Rousset, D. Farrusseng, *Chem. Commun.* **2013**, *49*, 8507 – 8509.
[57] T. L. Cui, W. Y. Ke, W. B. Zhang, H. H. Wang, X. H. Li, J. S. Chen, *Angew. Chem. Int. Ed.* **2016**, *55*, 9178 – 9182; *Angew. Chem.* **2016**, *128*, 9324 – 9328.
[58] C. Wang, L. Wang, J. Zhang, H. Wang, J. P. Lewis, F. S. Xiao, *J. Am. Chem. Soc.* **2016**, *138*, 7880 – 7883.
[59] S. Li, C. Aquino, L. Gueudré, A. Tuel, Y. Schuurman, D. Farrusseng, *ACS Catal.* **2014**, *4*, 4299 – 4303.
[60] S. Li, T. Boucheron, A. Tuel, D. Farrusseng, F. Meunier, *Chem. Commun.* **2014**, *50*, 1824 – 1826.
[61] S. Li, A. Tuel, J. L. Rousset, F. Morfin, M. Aouine, L. Burel, F. Meunier, D. Farrusseng, *ChemNanoMat* **2016**, *2*, 534 – 539.
[62] N. Ren, Y. H. Yang, S. Jiang, Y. H. Zhang, H. L. Xu, Z. Gao, Y. Tang, *J. Catal.* **2007**, *251*, 182 – 188.
[63] N. Ren, Y. H. Yang, Y. H. Zhang, Q. R. Wang, Y. Tang, *J. Catal.* **2007**, *246*, 215 – 222.

[64] J. Zhang, L. Wang, B. Zhang, H. Zhao, U. Kolb, Y. Zhu, L. Liu, Y. Han, G. Wang, C. Wang, D. S. Su, B. C. Gates, F. S. Xiao, *Nat. Catal.* **2018**, *1*, 540 – 546.

[65] J. Zhang, L. Wang, Y. Shao, Y. Wang, B. C. Gates, F. S. Xiao, *Angew. Chem. Int. Ed.* **2017**, *56*, 9747 – 9751; *Angew. Chem.* **2017**, *129*, 9879 – 9883.

[66] J. Zhang, L. Wang, L. Zhu, Q. Wu, C. Chen, X. Wang, Y. Ji, X. Meng, F. S. Xiao, *ChemSusChem* **2015**, *8*, 2867 – 2871.

[67] M. Choi, Z. Wu, E. Iglesia, *J. Am. Chem. Soc.* **2010**, *132*, 9129 – 9137.

[68] T. Otto, S. I. Zones, E. Iglesia, *J. Catal.* **2016**, *339*, 195 – 208.

[69] Z. Wu, S. Goel, M. Choi, E. Iglesia, *J. Catal.* **2014**, *311*, 458 – 468.

[70] J. Gu, Z. Zhang, P. Hu, L. Ding, N. Xue, L. Peng, X. Guo, M. Lin, W. Ding, *ACS Catal.* **2015**, *5*, 6893 – 6901.

[71] Q. Wang, L. Wang, Z. Mi, *Catal. Lett.* **2005**, *103*, 161 – 164.

[72] B. Taylor, J. Lauterbach, W. N. Delgass, *Appl. Catal. A* **2005**, *291*, 188 – 198.

[73] L. Cumaranatunge, W. N. Delgass, *J. Catal.* **2005**, *232*, 38 – 42.

[74] S. T. Oyama, X. Zhang, J. Lu, Y. Gu, T. Fujitani, *J. Catal.* **2008**, *257*, 1 – 4.

[75] M. M. Mohamed, T. M. Salama, M. Ichikawa, *J. Colloid Interface Sci.* **2000**, *224*, 366 – 371.

[76] C. Wang, Z. Liu, L. Wang, X. Dong, J. Zhang, G. Wang, S. Han, X. Meng, A. Zheng, F. S. Xiao, *ACS Catal.* **2018**, *8*, 474 – 481.

[77] A. Laurent Djakovitch, K. Koehler, *J. Am. Chem. Soc.* **2001**, *123*, 5990 – 5999.

[78] A. K. Aboul-Gheit, S. M. Aboul-Fotouh, S. M. Abdel-Hamid, N. A. K. Aboul-Gheit, *J. Mol. Catal A* **2006**, *245*, 167 – 177.

[79] A. K. Aboul-Gheit, A. E. Awadallah, N. A. K. Aboul-Gheit, E.-S. A. Solyman, M. A. Abdel-Aaty, *Appl. Catal. A* **2008**, *334*, 304 – 310.

[80] W. Lu, W. Feng, J. Wang, *New J. Chem.* **2016**, *40*, 3019 – 3023.

[81] M. Sugioka, F. Sado, Y. Matsumoto, N. Maesaki, *Catal. Today* **1996**, *29*, 255 – 259.

[82] Y. Y. Sun, R. Prins, *Angew. Chem. Int. Ed.* **2008**, *47*, 8478 – 8481; *Angew. Chem.* **2008**, *120*, 8606 – 8609.

[83] J. M. García-Cortés, J. Pérez-RamíRez, M. J. Illán-Gómez, F. Kapteijn, J. A. Moulijn, S. M. N. D. Lecea, *Appl. Catal. B* **2001**, *30*, 399 – 408.

[84] A. Wang, L. Ma, C. Yu, T. Zhang, D. Liang, *Appl. Catal. B* **2003**, *40*, 319 – 329.

[85] Z. X. Gao, Q. Sun, H. Y. Chen, X. Wang, W. M. H. Sachtler, *Catal. Lett.* **2001**, *72*, 1 – 5.

[86] S. I. Woo, D. K. Kim, K. P. Yong, M. R. Kim, P. Decyk, *Catal. Lett.* **2003**, *85*, 69 – 72.

[87] T. M. Salama, R. Ohnishi, M. Ichikawa, *Chem. Commun.* **1997**, 105 – 106.

[88] V. Rico Pérez, J. M. García-Cortés, A. Bueno-López, *Chem. Eng. Sci.* **2013**, *104*, 557 – 564.

[89] K. C. Park, S. K. Ihm, *Appl. Catal. A* **2000**, *203*, 201 – 209.

[90] J. A. Martens, D. Verboekend, K. Thomas, G. Vanbutsele, J. Pérez Ramírez, J. P. Gilson, *Catal. Today* **2013**, *218 – 219*, 135 – 142.

[91] R. Brosius, P. J. Kooyman, J. C. Q. Fletcher, *ACS Catal.* **2016**, *6*, 7710 – 7715.

[92] G. Burnens, C. Bouchy, E. Guillon, J. A. Martens, *J. Catal.* **2011**, *282*, 145 – 154.

[93] M. Y. Kim, J. K. Kim, M. E. Lee, S. Lee, M. Choi, *ACS Catal.* **2017**, *7*, 6256 – 6267.

[94] M. Shekhar, J. Wang, W.-S. Lee, W. D. Williams, S. M. Kim, E. A. Stach, J. T. Miller, W. N. Delgass, F. H. Ribeiro, *J. Am. Chem. Soc.* **2012**, *134*, 4700 – 4708.

[95] "The Influence of Particle Size on the Catalytic Properties of Supported Metals": M. Che, C. O. Bennett, in *Advances in Catalysis*, *Vol. 36* (Eds.: D. D. Eley, H. Pines, P. B. Weisz), Academic Press, San Diego, **1989**, pp. 55 – 172.

[96] M. Haruta, N. Yamada, T. Kobayashi, S. Iijima, *J. Catal.* **1989**, *115*, 301 – 309.

[97] a) M. Flytzani-Stephanopoulos, B. C. Gates, *Annu. Rev. Chem. Biomol.* **2012**, *3*, 545 – 574; b) H. Hosseiniamoli, G. Bryant, E. M. Kennedy, K. Mathisen, D. Nicholson, G. Sankar, A. Setiawan, M. Stockenhuber, *ACS Catal.* **2018**, *8*, 5852 – 5863.

[98] Y. Lykhach, S. M. Kozlov, T. Skála, A. Tovt, V. Stetsovych, N. Tsud, F. Dvořák, V. Johánek, A. Neitzel, J. Mysliveček, *Nat. Mater.* **2016**, *15*, 284 – 288.

[99] Y. Lei, F. Mehmood, S. Lee, J. Greeley, B. Lee, S. Seifert, R. E. Winans, J. W. Elam, R. J. Meyer, P. C. Redfern, D. Teschner, R. Schlögl, M. J. Pellin, L. A. Curtiss, S. Vajda, *Science* **2010**, *328*, 224 – 228.

[100] T. W. Hansen, A. T. Delariva, S. R. Challa, A. K. Datye, *Acc. Chem. Res.* **2013**, *46*, 1720 – 1730.

[101] S. R. Challa, A. T. Delariva, T. W. Hansen, H. Stig, S. Jens, P. L. Hansen, G. Fernando, A. K. Datye, *J. Am. Chem. Soc.* **2011**, *133*, 20672 – 20675.

[102] X. Y. Yang, Z. Q. Li, B. Liu, A. Klein-Hofmann, G. Tian, Y. F. Feng, Y. Ding, D. S. Su, F. S. Xiao, *Adv. Mater.* **2006**, *18*, 410 – 414.

[103] W. M. H. Sachtler, *Acc. Chem. Res.* **1993**, *26*, 383 – 387.

[104] See Ref. [53].

[105] R. E. Jentoft, M. Tsapatsis, M. E. Davis, B. C. Gates, *J. Catal.* **1998**, *179*, 565 – 580.

[106] P. B. Weisz, *Microporous Mesoporous Mater.* **2000**, *35*, 1 – 9.

[107] P. B. Weisz, V. J. Frilette, *J. Phys. Chem.* **1960**, *64*, 382.

[108] P. B. Weisz, *Pure Appl. Chem.* **1980**, *52*, 2091 – 2103.

[109] S. M. Csicsery, *Zeolites* **1984**, *4*, 202 – 213.

[110] B. Smit, T. L. M. Maesen, *Chem. Rev.* **2008**, *108*, 4125 – 4184.

[111] J. Weitkamp, L. Puppe, T. Chemie, *Catalysis and Zeolites*, Springer, Berlin, **1999**.

[112] B. H. Wu, H. Q. Huang, J. Yang, N. F. Zheng, G. Fu, *Angew. Chem. Int. Ed.* **2012**, *51*, 3440 – 3443; *Angew. Chem.* **2012**, *124*, 3496 – 3499.

[113] S. T. Marshall, M. O'Brien, B. Oetter, A. Corpuz, R. M. Richards, D. K. Schwartz, J. W. Medlin, *Nat. Mater.* **2010**, *9*, 853 – 858.

[114] P. Barbaro, F. Liguori, N. Linares, C. M. Marrodan, *Eur. J. Inorg. Chem.* **2012**, 3807 – 3823.

[115] S. Sartipi, M. Makkee, F. Kapteijn, J. Gascon, *Catal. Sci. Technol.* **2014**, *4*, 893 – 907.

[116] G. Wang, Q. Liu, W. Su, X. Li, Z. Jiang, X. Fang, C. Han, C. Li, *Appl. Catal. A* **2008**, *335*, 20 – 27.

[117] Y. Chai, S. Liu, Z. J. Zhao, J. Gong, W. Dai, G. Wu, N. Guan, L. Li, *ACS Catal.* **2018**, *8*, 8578 – 8589.

[118] D. Santi, S. Rabl, V. Calemma, M. Dyballa, M. Hunger, J. Weitkamp, *ChemCatChem* **2013**, *5*, 1524 – 1530.

[119] T. L. Lohr, T. J. Marks, *Nat. Chem.* **2015**, *7*, 477 – 482.

[120] M. J. Climent, A. Corma, S. Iborra, M. J. Sabater, *ACS Catal.* **2014**, *4*, 870 – 891.

[121] J. Zecevic, G. Vanbutsele, K. P. de Jong, J. A. Martens, *Nature* **2015**, *528*, 245 – 248.

[122] X. Yang, A. Varma, *ACS Energy Lett.* **2016**, *1*, 963 – 968.

[123] K. C. Nicolaou, D. J. Edmonds, P. G. Bulger, *Angew. Chem. Int. Ed.* **2006**, *45*, 7134 – 7186; *Angew. Chem.* **2006**, *118*, 7292 – 7344.

[124] N. T. Cuong, H. M. T. Nguyen, M. T. Nguyen, *Phys. Chem. Chem. Phys.* **2013**, *15*, 15404 – 15415.

[125] a) G. A. Filonenko, R. van Putten, E. J. M. Hensen, E. A. Pidko, *Chem. Soc. Rev.* **2018**, *47*, 1459 – 1483; b) K. Khivantsev, N. R. Jaegers, L. Kovarik, J. C. Hanson, F. Tao, Y. Tang, X. Zhang, I. Z. Koleva, H. A. Aleksandrov, G. N. Vayssilov, Y. Wang, F. Gao, J. Szanyi, *Angew. Chem. Int. Ed.* **2018**, *57*, 16672 – 16677; *Angew. Chem.* **2018**, *130*, 16914 – 16919.

[126] a) L. H. Chen, X. Y. Li, G. Tian, Y. Li, J. Rooke, G. S. Zhu, Q. S. Lun, X. Y. Yang, B. L. Su, *Angew. Chem. Int. Ed.* **2011**, *50*, 11156 – 11161; *Angew. Chem.* **2011**, *123*, 11352 – 11357; b) S.

Xiao, Y. Lu, X. Li, B. Y. Xiao, L. Wu, J. P. Song, Y. X. Xiao, S. M. Wu, J. Hu, Y. Wang, G. G. Chang, G. Tian, S. Lenaerts, C. Janiak, X. Y. Yang, B. L. Su, *Chem. Eur. J.* **2018**, *24*, 13246 – 13252; c) Y. Dong, S. Y. Chen, Y. Lu, Y. X. Xiao, J. Hu, S. M. Wu, Z. Deng, G. Tian, G. G. Chang, J. Li, S. Lenaerts, C. Janiak, X. Y. Yang, B. L. Su, *Chem. Asian J.* **2018**, *13*, 1609 – 1615.

[127] C. M. A. Parlett, M. A. Isaacs, S. K. Beaumont, L. M. Bingham, N. S. Hondow, K. Wilson, A. F. Lee, *Nat. Mater.* **2016**, *15*, 178 – 182.

[128] D. R. Rolison, C. A. Bessel, *Acc. Chem. Res.* **2000**, *33*, 737 – 744.

[129] X. Zhang, X. Ke, H. Zhu, *Chem. Eur. J.* **2012**, *18*, 8048 – 8056.

[130] P. Sumant, V. P. Vinod, M. Kausik, K. Ashavani, R. Mala, R. V. Chaudhari, S. Murali, *Biotechnol. Bioeng.* **2004**, *85*, 629 – 637.

[131] a) G. Li, S. Zhao, Y. Zhang, Z. Tang, *Adv. Mater.* **2018**, *30*, 1800702; b) M. Meilikhov, K. Yusenko, D. Esken, S. Turner, G. Van Tendeloo, R. A. Fischer, *Eur. J. Inorg. Chem.* **2010**, 3701 – 3714; c) A. Dhakshinamoorthy, H. Garcia, *Chem. Soc. Rev.* **2012**, *41*, 5262 – 5284; d) H. R. Moon, D. W. Lim, M. Paik Suh, *Chem. Soc. Rev.* **2013**, *42*, 1807 – 1824; e) P. Falcaro, R. Ricco, A. Yazdi, I. Imaz, S. Furukawa, D. Maspoch, R. Ameloot, J. D. Evans, C. J. Doonan, *Coord. Chem. Rev.* **2016**, *307*, 237 – 254; f) J. Yu, C. Mu, B. Yan, X. Qin, C. Shen, H. Xue, H. Pang, *Mater. Horiz.* **2017**, *4*, 557 – 569.

[132] Q. Fu, F. Yang, X. Bao, *Acc. Chem. Res.* **2013**, *46*, 1692 – 1701.

Manuscript received: January 1, 2019
Accepted manuscript online: March 1, 2019
Version of record online: June 13, 2019

